Vol. 41, No. 3 (2019) 452-462, DOI: 10.24874/ti.2019.41.03.15

Tribology in Industry

www.tribology.rs

RESEARCH

Characterization of the Tribological Properties of Bismuth-titanate Coatings Synthesized by Sol-gel on 316L Stainless Steel Substrates

J. Bautista-Ruiz[a], A. Chaparro[b], J.J. Olaya[c]

[a]*Universidad Francisco de Paula Santander, Avenida Gran Colombia 12E-96, San José de Cúcuta, Colombia,*
[b]*Universidad ECCI, carrera 19 No. 49-20, Bogotá, Colombia,*
[c]*Universidad Nacional de Colombia, carrera 30 No. 45ª-03, Bogotá, Colombia.*

Keywords:

Tribological
Wear
Sol-gel
Bimuth-titanate
Thin films

Corresponding author:

Jorge Bautista-Ruiz
Universidad Francisco de Paula Santander, Avenida Gran Colombia 12E-96 B. Colsag, San José de Cúcuta, Colombia.
E-mail: jorgebautista@ufps.edu.co

A B S T R A C T

The objective of this investigation was to obtain ceramic coatings of bismuth titanate by Sol-gel synthesis on 316L stainless steel substrates using bismuth nitrate pentahydrate (III) and titanium tetrabutoxide as precursors. The characterization focused on determining wear rates, coefficients of friction, adhesion, nano-hardness, and thickness of the coatings, depending on the concentration of the precursors, the speed of rotation and the number of layers. It is concluded that the sol presents favorable conditions for their potential application as coatings on metallic substrates.

1. INTRODUCTION

The sol-gel method allows the shaping of ceramic materials from polymerization routes of components in a liquid state, sol, at room temperature [1]. This method is considered simple, easy to adopt, low cost, easy preparation, physical and chemical homogeneity, low synthesis temperature and high purity of the final product [2,3].

The manufacture of thin films of metal oxides by the sol-gel method is applicable to metal substrates (stainless steel, aluminum, and their alloys) with various geometric shapes. The applications of these coatings cover industrial purposes [5] and sanitary. For example, they improve the resistance to corrosion [4-6], in the protection of orthopedic implants and biomedical applications [7-9], in the improvement of the resistance to wear and tribological properties [10-15].

There is a growing interest in the mechanical industry to look for alternatives that reduce the wear of metallic materials and decrease one of the main causes of loss of profitability [16]. Reducing the wear of metal parts used as joints

is also important in the field of biomedical applications. Currently, research is being conducted on the benefits that materials such as bismuth and its alloys can offer in reducing wear rates. Bismuth has growing commercial importance, is not considered toxic and presents a minimal threat to the environment [17].

In large part of the development of the industrial framework and in biomedical applications, AISI 316L stainless steel is widely used and is characterized by good resistance to corrosion, malleability, weldability, and biocompatibility. These properties make it a functional and versatile material in the chemical, naval, petrochemical, pharmaceutical, food and biomedical industries [18,19]. Stainless steel generally exhibits poor tribological properties limiting its applications requiring little wear [20]. In several socioeconomic sectors, it is expensive to replace pieces made of stainless steel. In the mechanical sector, this problem could be solved by developing protective coatings for abrasion and erosion [21], instead of conventional lubricants where the application of lubricants in extreme environments is not feasible because it entails many difficulties [21,22].

The synthesis of coatings via sol-gel on metallic substrates for applications that allow reducing the wear, the compounds with the formula $Bi_{12}MO_{20}$ (M = Si, Ge, Ti, Pb, Mn $B_{1/2}$ $P_{1/2}$), called sillenites, which can be considered promising materials [23,24].

The objective of this investigation was to obtain ceramic coatings of bismuth titanate by Sol-gel synthesis on 316L stainless steel substrates using bismuth nitrate pentahydrate (III) and titanium tetrabutoxide as precursors. The characterization focused on determining wear rates, coefficients of friction, adhesion, nano-hardness, and thickness of the coatings, depending on the concentration of the precursors, the speed of rotation and the number of layers.

2. METHODS AND MATERIALS

The methodology of synthesis of the stable sols is shown in Fig. 1. Before starting the process, it is necessary to vacuum dry at 70 °C for 96 hours the Bi $(NO_3)_3$ $5H_2O$ to decrease the amount of water in the final compound. Two solutions labeled A and B are established. In solution A, the bismuth nitrate was dissolved in acetic acid for 2 hours at room temperature. Solution B contained titanium (IV) butoxide and ethanolamine under stirring for 3 hours at room temperature. When the agitation times of solutions A and B have been completed, they are mixed. Finally, the ethanolamine was added until a pH = 4 was reached to avoid hydrolysis of the bismuth ions. The amounts and molar concentrations of the precursors used in this study are indicated in Table 1.

Table 1. Amounts and molar concentrations of the precursors.

Coating	$Ti(OBu)_4$ (ml)	$Bi(NO_3)$ (ml)	$C_2H_4O_2$ (ml)
{Bi-Ti/80-20}	50.44	36.32	100
{Bi-Ti/50-50}	18.16	52.24	
{Bi-Ti/20-80}	5.08	57.08	

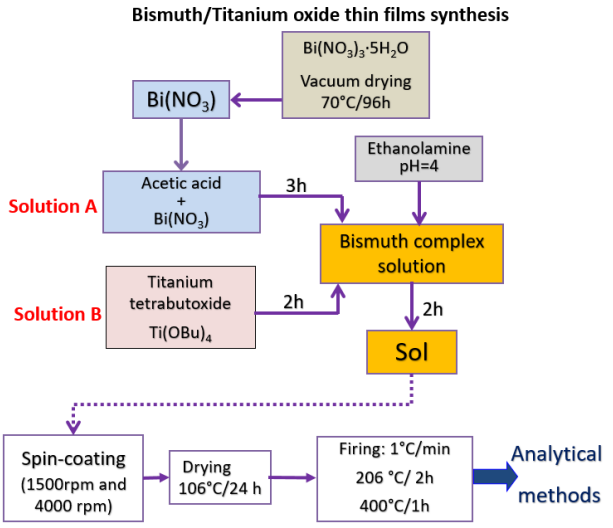

Fig. 1. Bismuth/Titanium and thin films synthesis.

316 L (SS) stainless steel pieces with dimensions of 2 cm x 2 cm x 0.4 cm were used as substrates. They were polished with abrasive papers of silicon carbide numbers 360, 500, 1000 and 1200, and alumina. After the polishing phase and to remove impurities, the substrates were washed in acetone and in an ultrasonic bath for 10 minutes.

The films were deposited on the substrate using the spin coating technique at speeds of 1500 rpm and 4000 rpm for 10 s, respectively.

Coatings were formed in monolayer and bilayer. For the monolayers, the films are subjected to a

drying process for 24 hours at 106 °C. For the sintering, the coatings were fixed at a heating rate of 1 °C/min. The thermal process is established from 25 °C to 206 °C, stabilizing for two hours. The process continues until reaching 400 ° C and is maintained at this temperature for one hour. Finally, the temperature decreases to 25 °C. This same sintering program was maintained for the bilayers.

The wear test was developed under the ASTM G99 standard, the equipment used was a CETR-UMT-2-110 tribometer, using a ball of alumina (Al_3O_2) of radius 3 mm, with a load of 400g, a speed of 689 rev/s, varying the traveled distances of 1310m in a track radius of 5.5 mm.

To test the adhesion of films deposited on 316L SS, the adhesion test was developed with the CSM Revetest Xpress Scratch Tester. The applied load increases progressively from 0 to 20N at a scratch length of 8mm, a Rockwell indenter C 200 μm radius, the scratching speed was 10 mm/min at a load rate of 100N/min.

The nano-hardness and the modulus of elasticity of the coatings were measured in a Hysitron TI 950 tribo-indentant equipment. A Berkovich diamond tip with a minimum penetration depth of 30 nm was used. The values of hardness and elastic modulus were determined from the load-displacement curves by the Oliver-Pharr method [25]. The samples are analysed in the configuration of very low forces to avoid displacements during the topographic survey. The maximum load used was 10000 μN.

To measure the thickness, a DEKTAK 150 profilometer with 6 Å repeatability was used. The measurements were made with a 600 μm sweep, lasting 30 s, applying a force of 1 mg, with valleys and ridges, and a resolution of 0.067 μm / sample.

3. RESULTS

3.1 Thickness

In Table 2, the thickness values for the coatings of the BTO system are indicated as a function of the concentration, the number of layers and the speed of forming or centrifugation.

Table 2. Thickness values for BTO coatings.

Coating	Layer	Spin speed	
		1500 rpm	4000 rpm
		Thickness (nm)	
{Bi-Ti/80-20}	Monolayer	268.01	155.84
	Bilayer	469.65	393.92
{Bi-Ti/50-50}	Monolayer	188.50	108.06
	Bilayer	263.69	156.03
{Bi-Ti/20-80}	Monolayer	180.80	93.48
	Bilayer	267.59	236.24

The information recorded in Table 2, it can be concluded that: 1) the centrifugation speeds have a significant influence on the final thickness of the coatings, thus: high spin speeds allow the obtaining coatings with low thicknesses, in comparison with films obtained at high speeds (4000 rpm). 2) The number of layers also influences the final results; increasing the number of layers increases the final thickness of the film. The effect of the concentration of the precursors determines the value of the final thickness. The thinnest coatings are manifested in the monolayer of the concentration {Bi-Ti/20-80} at 4000 rpm, 93 nm. The greatest thicknesses are observed in the bilayer {Bi-Ti/40-60} with 497 nm. The final thickness of the film is influenced by the growth of the Bi and Ti oxides on the surface of the films.

3.2 Wear

Figures 2 and 3 show the wear rates of the coatings of the bismuth-titanate system (BTO) as a function of the molar concentration, of the sol and the spin speeds and the number of layers.

The comparison between monolayers and bilayers at 1500 rpm according to the three concentrations studied is indicated in Fig. 2. In this figure and for the graph labeled as a) it is observed, for monolayer coatings, that high concentrations of titanium tetrabutoxide precursor of titanium provide coatings with low wear rates. This same trend can be seen in figure b) for bilayer coatings. When comparing graphs, a) and b), a higher wear rate for the monolayers is evidenced.

Figure 3 compares the values of the wear rates for monolayers and bilayers formed at 4000 rpm, varying the concentrations of the precursors of which the films were made. With respect to the monolayers, figure a), high

concentrations of bismuth nitrate precursor of bimuth provide coatings with high wear rates. In bilayer coatings, the trend in the values of wear rates as a function of the concentration of the precursors is not as relevant.

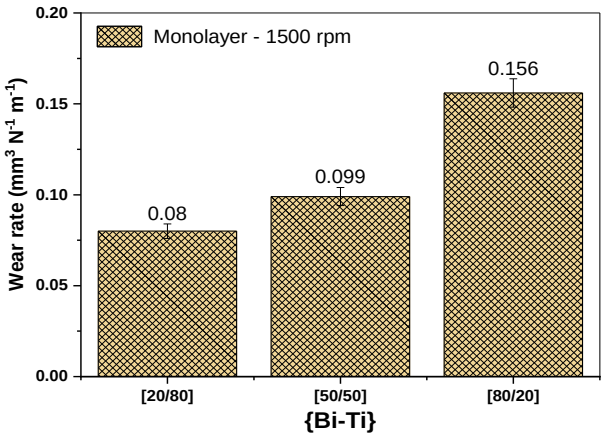

a)

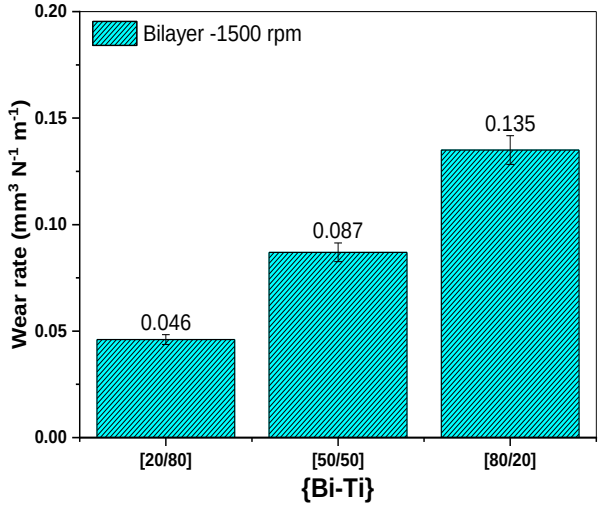

b)

Fig. 2. Wear rates for BTO system coatings shaped at 1500 rpm. a) monolayer and b) bilayer.

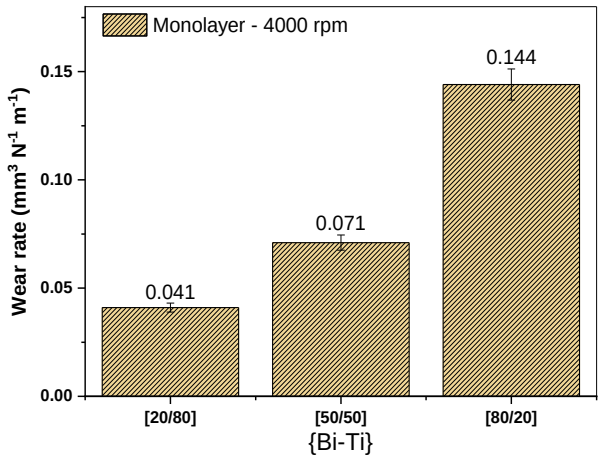

a)

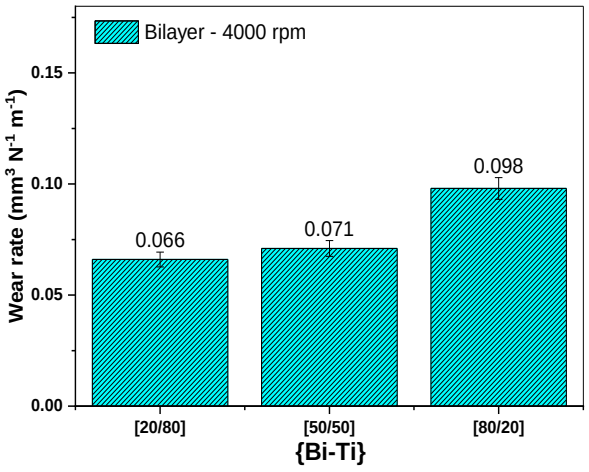

b)

Fig. 3. Wear rates for BTO system coatings shaped at 4000 rpm. a) monolayer and b) bilayer.

From the study, it is concluded that monolayer coatings at speeds of 4000 rpm show the best results in terms of low wear rates. The wear rate for the 316L substrate is 0.33 mm^3 N^{-1} m^{-1}. Comparing with the results obtained for the five concentrations in relation to the number of layers applied over the substrate and varying the speeds of centrifugation, it is concluded that all the coatings of the bismuth-titanate system (BTO) offer protection to the substrate by indicating wear rates lower than that reported for stainless steel 316L.

Figures 4 and 5 show the three-dimensional reconstruction of the wear traces for the coatings of the bismuth-titanate system (BTO) as a function of the molar concentration of the sol, the spin speeds and the number of layers. According to the results, wear particles distributed around the tracks are observed. The particles sometimes showed a very uniform distribution on both sides of the footprint, while at other times they did not, accumulating more to one side than to the other.

3.3 Coefficient of friction

In figures 6 to 8, the graphs of the coefficient of friction of coatings of the BTO system in its three molar concentrations are shown varying the number of layers and the speed of obtaining. The values of the coefficients of friction were estimated between the contact surfaces: coating - sphere of alumina.

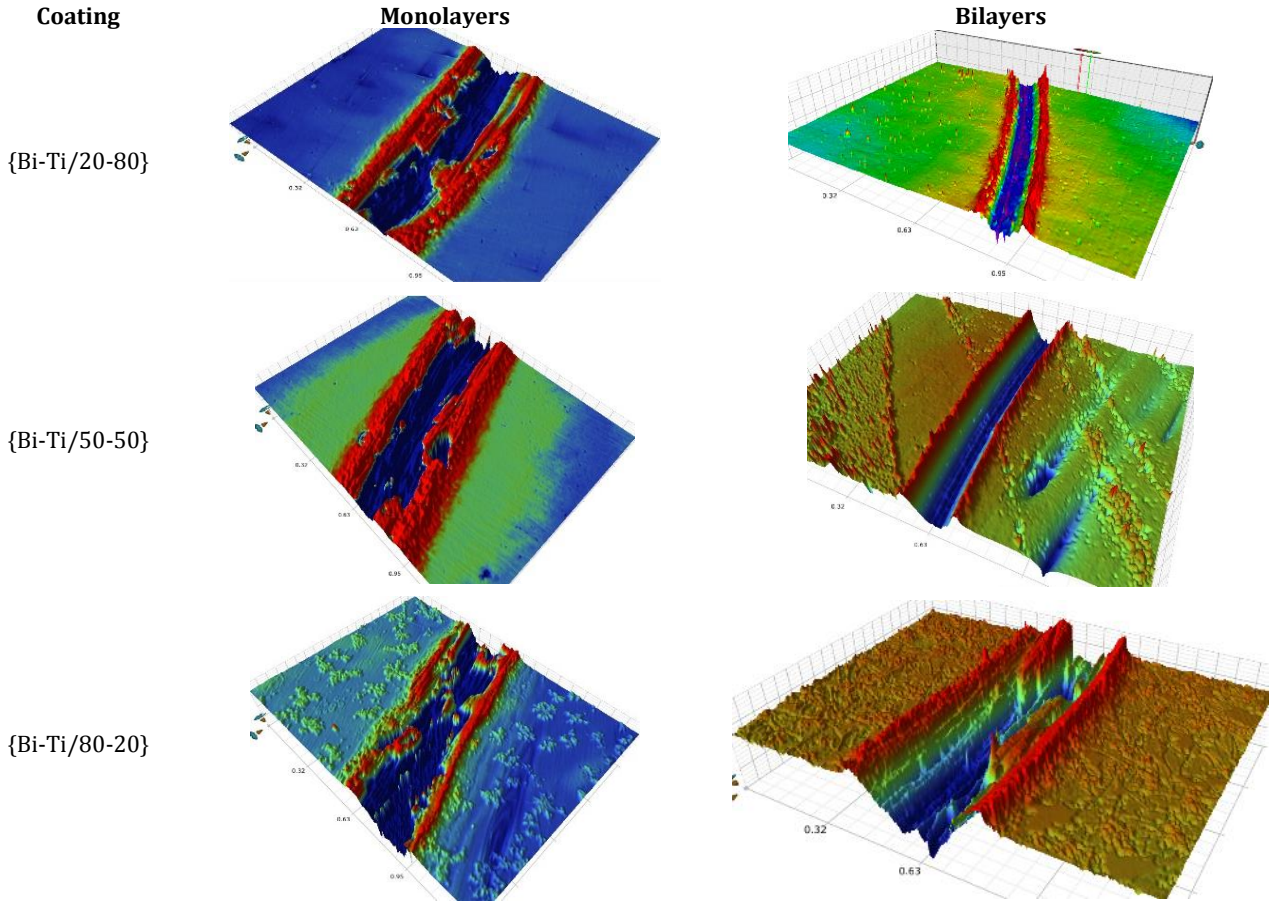

Fig. 4. Wear traces for the coatings of the BTO system for monolayers and bilayers at 1500 rpm.

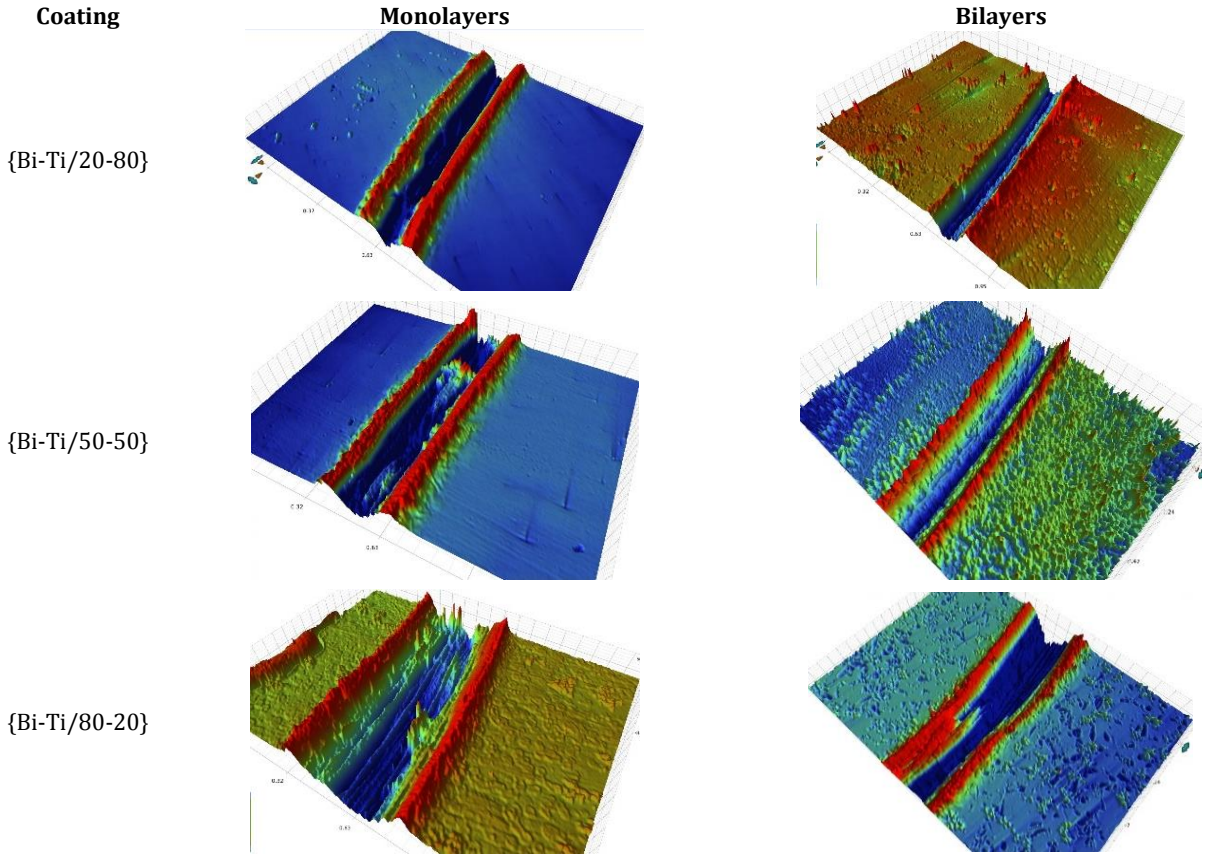

Fig. 5. Wear traces for the coatings of the BTO system for monolayers and bilayers at 4000 rpm.

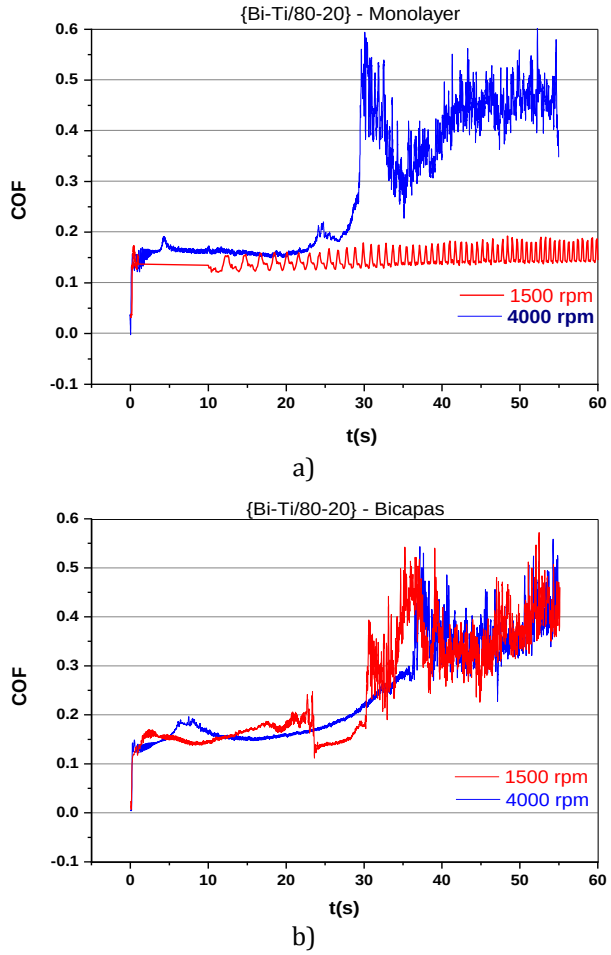

Fig. 6. Coefficients of friction for coatings {Bi-Ti/20-80}, a) monolayer and b) bilayer.

The curves of the coefficient of friction for the films of the concentration {Bi-Ti/20-80} in monolayer and bilayer at speeds of centrifugation of 1500 rpm and 4000 rpm can be seen in Fig. 6. In curve a) it can be seen that the coefficient of friction of the monolayer film at 1500 rpm takes COF values between 0.13 and 0.15 and remains constant until the end of the test. For the monolayers at 4000 rpm, it is evident that the COF adopts values between 0.16 and 0.18 during the first 25 s of the test. During the last 30 seconds of the test, the COF value is increased, oscillating between 0.18 and 0.45, due to the existence of debris removed by the wear in the own processes of the adhesive wear. In Fig. 6b the friction coefficient curves for bilayers are evident. Regarding the bilayer at 1500 rpm it can be seen that, during the initial 10 seconds of the test, the COF value assumes values between 0.14 and 0.16. In the last 45 seconds, the COF has great variations reaching 0.45 on average. This behavior is explained by the adhesive wear and detachment of the film.

The determination of the COF for the films in concentration {Bi-Ti/50-50} are indicated in Fig. 7. With respect to the bilayers, Fig. 7b, there is no significant difference in the behavior of the graph as in the values of the COF. According to the records, it can be shown that the average value of the COF is 0.15 and no effect of the centrifugation speed with which the films were formed is revealed. Regarding the monolayers, it is possible to affirm that the behaviors of the graphs, during the time that the test took, do not show greater stability. It is possible to consider a COF value of 0.13 to 2.0 for the film at 4000 rpm and 0.14 to 2.0 for the coating at 1500 rpm, during the first 15 seconds of testing. In the remaining 40 seconds, the COF values reach 0.35 in both cases, with a rather irregular graphic behavior (Fig. 7a).

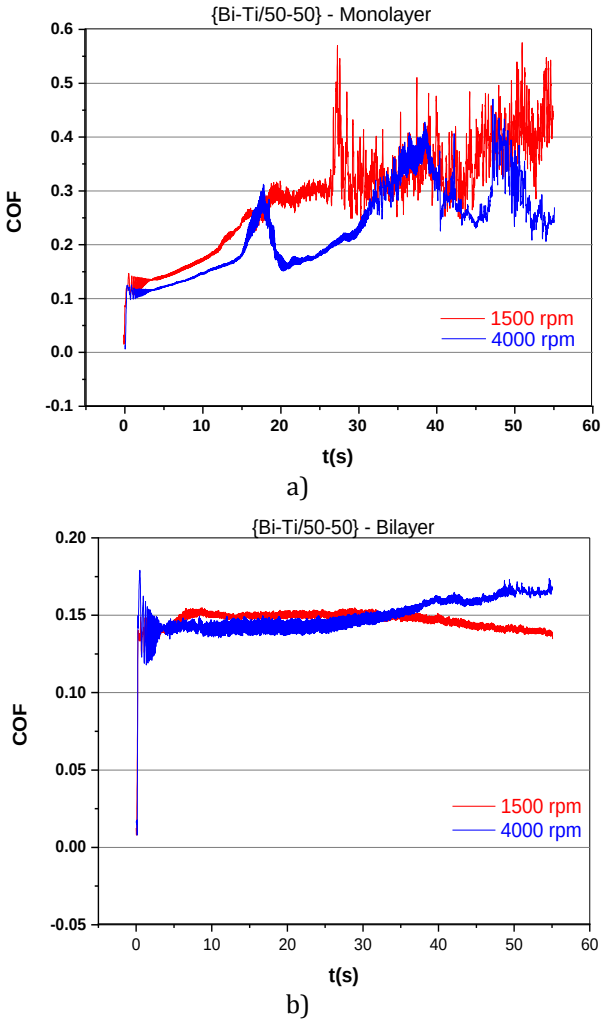

Fig. 7. Coefficients of friction for coatings {Bi-Ti/50-50}, a) monolayer and b) bilayer.

Finally, Fig. 8 indicates the graphs of the coefficients of friction as a function of the test

time for monolayer and bilayer coatings obtained at speeds of 1500 rpm and 4000 rpm for a coating {Bi-Ti/80-20}. These speeds were selected in the process of forming the films using the spin-coating technique. For monolayers at 4000 rpm, a constant COF value between 0.14 and 0.18 is observed for the first 30 seconds of the test. For the last 25 seconds of the test, the erratic behavior of the graph is observed, the estimated value of the COF is 0.25 on average. As for the monolayer at 1500 rpm, the graph shows a COF between 0.13 to 0.20 in the initial 20 seconds of testing. In the final 35 seconds, the test takes, the graph shows that the COF value ranges between 0.20 and 0.4. Regarding the bilayers, it is observed that the graphs of COF fluctuate during all the time that is needed to develop the trial with the manifestation of abrupt changes in them. The COF values for the bilayer at 4000 rpm are estimated at 0.17 and for the bilayer, at 1500 rpm the COF value is 0.15 on average.

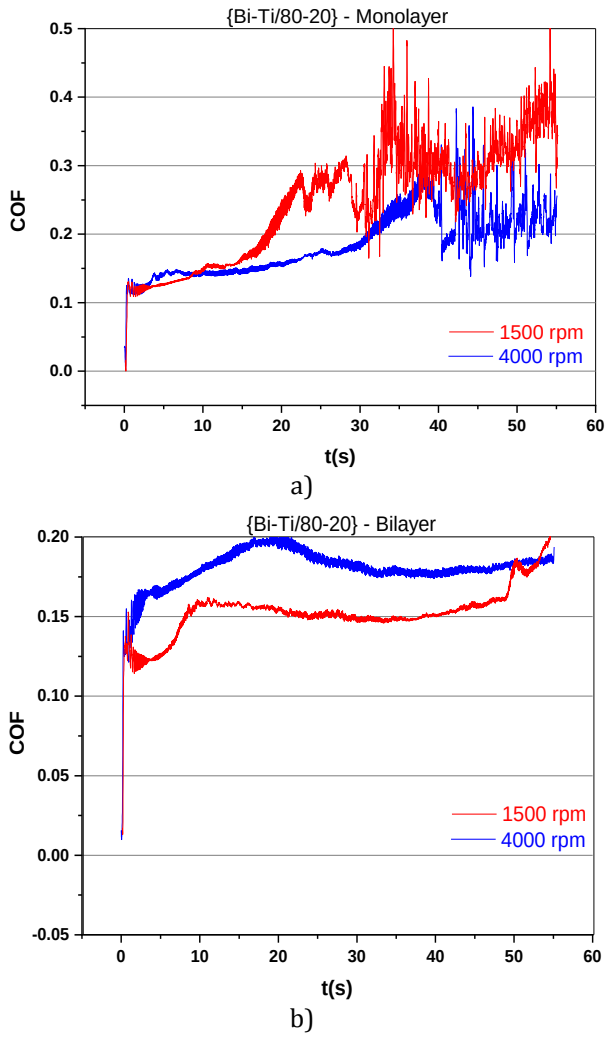

Fig. 8. Coefficients of friction for coatings {Bi-Ti/80-20}, a) monolayer and b) bilayer.

From the study of the coefficient of friction for the films obtained from the BTO system by varying the number of layers and speeds of centrifugation, it can be concluded that the abrupt variations of the coefficients of friction may be due to the existence of debris removed by wear due to the processes of the adhesive wear. Also, by the processes related to adhesive wear and film release. The very large fluctuations that appear in the graphs, possibly due to the appearance of wear particles that generate the abrupt increase in the friction force between the surfaces in contact and when they are expelled from the contact, the friction force decreases. In the tests, no wear of the alumina ball was observed.

3.4 Adhesion

Adhesion occurs when two surfaces are permanently joined due to forces present between them. The strength of adhesion usually originates in the molecular bonds between the coating, in this case, BTO; and the substrate. The forces of union between two surfaces vary in magnitude according to their origin: chemical, electrostatic, van der Waals forces, mechanical anchoring, capillarity or combinations of these. In addition to the adhesion forces, the stability of the substrate-coating interface is conditioned by the residual stresses.

Figures 9 to 12 show the photographs, at 200X, of the scratch marks of the coatings of the BTO system as a function of the number of layers applied to the substrate and the speed of centrifugation. The scratch test was developed under the ASTM C1624-05 standard. Only the most representative behaviors are shown.

In general, in all coatings, the appearance of the first faults correlated with the load Lc1 is observed, which represents the cohesive load. The second fault called Lc2 corresponds to the lifting or rolling of the film and the total failure of the coating. Internal transverse cracking caused by normal loading and displacement of the indenter is also observed. This behavior can be explained from the point of view of the ceramic nature of the BTO system films. For all the coatings it was found: that the first critical load LC1 is between 3.0 and 3.5N and the second critical load, Lc2, is around 5 N, there are no significant variations between coatings.

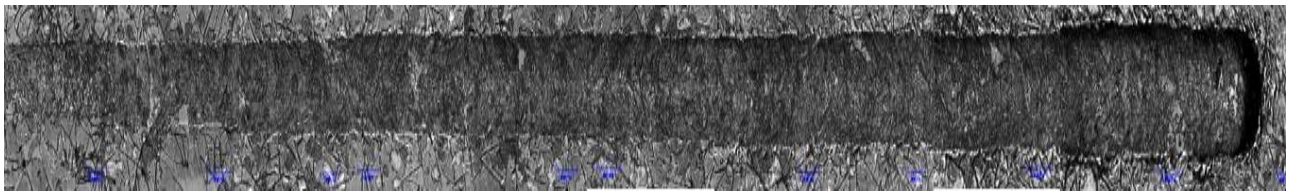

Fig. 9. Scoring footprint for coatings {Bi-Ti/80-20} in Bilayer at 1500 rpm.

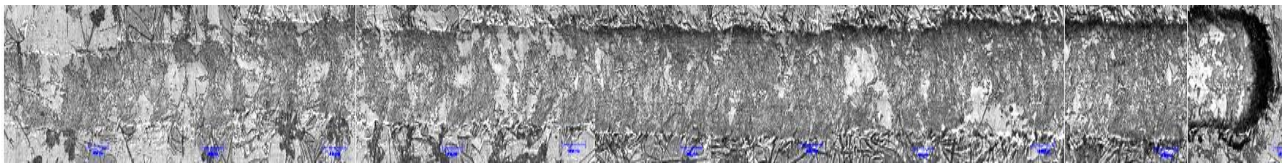

Fig. 10. Scoring footprint for coatings {Bi-Ti/80-20} in Bilayer at 4000 rpm.

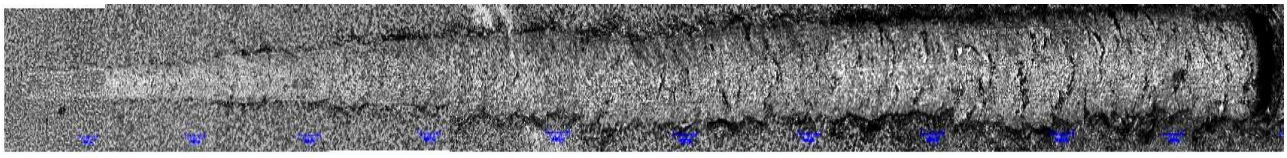

Fig. 11. Scoring footprint for coatings {Bi-Ti/50-50} in Bilayer at 4000 rpm.

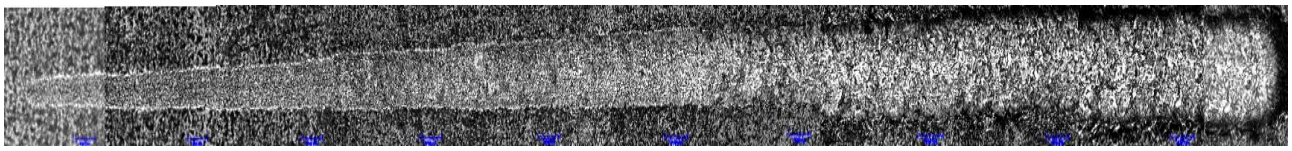

Fig. 12. Scoring footprint for coatings {Bi-Ti/20-80} in Bilayer at 1500 rpm.

3.5 Mechanical properties

Typical load-displacement curves for the thin films of the BTO system obtained for monolayers and bilayers, obtained at a spin speed of 1500 rpm are shown in Fig. 13. The load-displacement response obtained by nano-indentation contains information about the elastic deformation and plastic deformation of the coatings. The information related to the mechanical properties, such as hardness and Young's modulus, can be easily extracted from the load-displacement curves. The first observed inflection, both in the load and discharge curves, is related to the nonlinear relationship that manifests between the load and the deformation.

In Fig. 13, part a), the load corresponds to an elasto-plastic deformation and is characterized by the elasto-plastic properties of the material. The discharge generally represents a pure elastic behavior. The discharge curve does not follow a linear law, because during the removal of the indenter, the elastic relaxation leads to a variation of the shape of the footprint and at the same time of the contact surface. All the curves follow the same trajectory in the initial load segment until reaching approximately 5000 μN. This indicates that, initially, the test is a hardness test and is identical for the coatings in the three concentrations. No discontinuities are observed in the displacement of the tip, this allows to affirm that during the test no nucleation or growth was created cracks observed after the indentation, nor sudden jumps that give indication of results of bad adhesion of the films to the substrate.

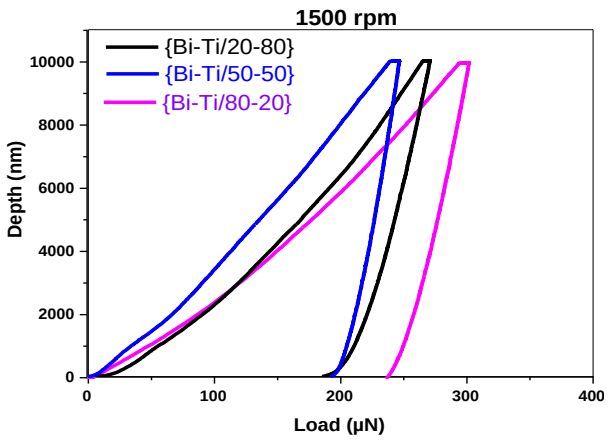

a)

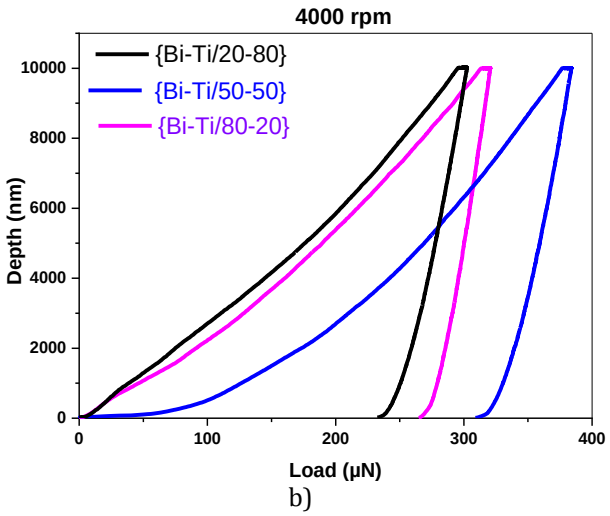

Fig. 13. Nano-indentation curves for BTO system coatings, a) Monolayers at 1500 rpm and b) bilayers at 1500 rpm.

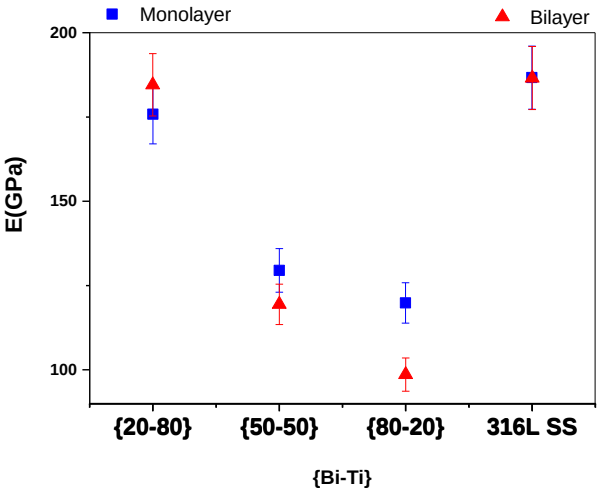

Fig. 14. Graph of the modulus of elasticity for coatings of the BTO system at 1500 rpm.

Figure 14 shows the values of modulus of elasticity and hardness for coatings in monolayer and bilayer at centrifugation speeds of 1500 rpm and 4000 rpm for the three molar concentrations studied. With respect to the modulus of elasticity, it was found that the films with the highest concentration are the most rigid with values a little lower than that reported for the substrate and that the number of layers deposited on the substrate does not have a marked influence on the final score. With respect to the hardness results (Fig. 15), it is established that all the studied coatings improve in this property with respect to the substrate. According to the obtained results, a proportional tendency is observed between the concentration of titanium tetrabutoxide present in the film and the hardness value thereof.

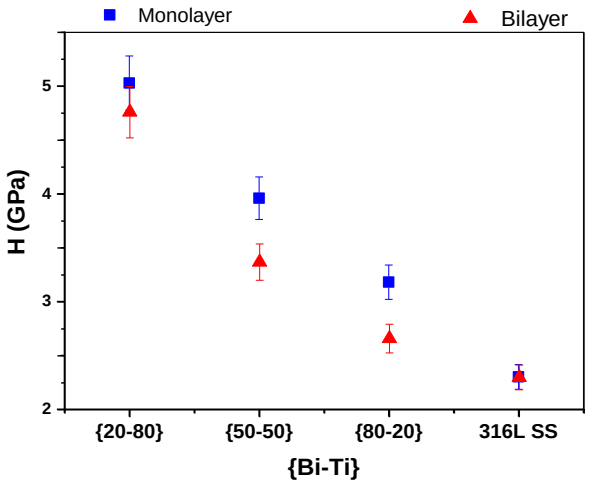

Fig. 15. Hardness graph for coatings of the BTO system at 1500 rpm.

In general terms, the results of nanoindentation it is possible to affirm: According to some investigations [21,23], the nano-hardness of the coatings decreases when the efforts change from compression to tension. It has also been found that the difference in the value of the elastic modulus of the constituent materials of the layers causes a decrease in the nano-hardness, i.e. the layers whose elastic modulus is low are not able to resist the generation and growth of cracks and therefore, the nano-hardness of the entire coating is negatively affected. Another factor determining the hardness of the coatings is its microstructure, as films with bismuth oxide and silicon formation were obtained. The diffusion of the atoms makes the interface between them not very well defined, therefore the composition shows a gradient, these phenomena allow dislocations to propagate in the layers allowing hardness to decrease.

4. CONCLUSIONS

Comparing with the wear results obtained for the three concentrations in relation to the number of layers applied to the substrate and varying the spin speeds it is concluded that all the coatings of the BTO system offer protection to the substrate by indicating wear rates lower than that reported for the 316L stainless steel.

From the study of the coefficient of friction for the films obtained from the BTO system by varying the number of layers and speeds of centrifugation, it can be concluded that the abrupt variations of the coefficients of friction may be

due to the existence of debris removed by wear due to the processes of the adhesive wear. Also, for the processes related to adhesive wear and film release. The very large fluctuations that occur, are possibly due to the appearance of wear particles that generate the abrupt increase of the friction force between the surfaces in contact and when they are expelled from the contact, the force friction decreases. In the tests, no wear of the alumina ball was observed.

The results of nanoindentation establish that all the coatings studied improve in this property with respect to the substrate. According to the obtained results, a proportional tendency is observed between the concentration of titanium tetrabutoxide present in the film and the hardness value thereof.

The final thickness of the coatings is influenced by the spin speeds and the number of layers applied to the substrate.

Acknowledgement

Dr Jorge Bautista thanks the "Fondo de Investigaciones Universitarias FINU de la Universidad Francisco de Paula Santander" project number 032/ 2018.

Author Contributions: J Bautista-Ruiz performed the obtaining coatings; W. Aperador worked in measurements in wear and adhesion and J. Olaya performed the interpretation of the adhesion data and the respective analysis.

REFERENCES

[1] J. Bautista-Ruiz, W. Aperador, A. Delgado, M. Díaz-Lagos, *Synthesis and Characterization of Anticorrosive Coatings of SiO2 -TiO2 - ZrO2 Obtained from Sol-Gel Suspensions,* International Journal of Electrochemical Science, vol. 9, pp. 4144-4157, 2014.

[2] H. Uchiyama, T. Bando, H. Kozuka, *Effect of the amount of H_2O and HNO_3 in $Ti(OC_3H_7^i)_4$ solutions on the crystallization of sol-gel-derived TiO_2 films*, Thin Solid Films, vol. 669, no. 1, pp. 157-161, 2019, doi: 10.1016/j.tsf.2018.10.050

[3] C. Brinker, G. Scherer, *Sol–gel science: The physics and chemistry of sol–gel processing,* San Diego: Academic Press, 1990.

[4] B. Tlili, A. Barkaoui, M. Walock, *Tribology and wear resistance of the stainless steel. The sol–gel coating impact on the friction and damage*, Tribology International, vol. 102, pp. 348-354, 2016, doi: 10.1016/j.triboint.2016.06.004

[5] H. Cheraghi, M. Shahmiri, Z. Sadeghian, *Corrosion behavior of TiO_2–NiO nanocomposite thin films on AISI 316L stainless steel prepared by sol–gel method*, Thin Solid Films, vol. 552, pp. 289-296, 2012, doi: 10.1016/j.tsf.2012.07.125

[6] G. Ruhi, O.P. Modi, A.S.K. Sinha, I.B. Singh, *Effect of sintering temperatures on corrosion and wear properties of sol–gel alumina coatings on surface pre-treated mild steel*, Corrosion Science, vol. 50, iss. 3, pp. 639-649, 2008, doi: 10.1016/j.corsci.2007.10.002

[7] S.A. Omar, J. Ballarre, S.M. Ceré, *Protection and functionalization of AISI 316L stainless steel for orthopedic implants: hybrid coating and sol gel glasses by spray to promote bioactivity*, Electrochimica Acta, vol. 203, pp. 309-315, 2016, doi: 10.1016/j.electacta.2016.01.051

[8] S.M. Hosseinalipour, A. Ershad-langroudi, A. Nemati, A.M. Nabizade-Haghighi, *Characterization of sol–gel coated 316L stainless steel for biomedical applications*, Progress in Organic Coatings, vol. 67, iss. 4, pp. 371-374, 2010, doi: 10.1016/j.porgcoat.2010.01.002

[9] S. Rahoui, V. Turq, J.-P. Bonino, *Effect of thermal treatment on mechanical and tribological properties of hybrid coatings deposited by sol–gel route on stainless steel*, Surface and Coatings Technology, vol. 235, pp. 15-23, 2013, doi: 10.1016/j.surfcoat.2013.07.008

[10] A. Alvarez-Vera, H.M. Hdz-García, R. Muñoz-Arroyo, J.C. Diaz-Guillen, A.I. Mtz-Enriquez, J.L. Acevedo-Dávila, *Tribological study of a thin TiO_2 nanolayer coating on 316L steel*, Wear, vol. 376, pp. 1702-1706, 2017, doi: 10.1016/j.wear.2017.01.029

[11] C. Belon, M. Schmitt, S. Bistac, C. Croutxé-Barghorn, A. Chemtob, *Friction and wear properties of hybrid sol–gel nanocomposite coatings against steel: Influence of their intrinsic properties*, Applied Surface Science, vol. 257, iss. 15, pp. 6618-6625, 2011, doi: 10.1016/j.apsusc.2011.02.088

[12] I. Piwoński, K. Soliwoda, *The effect of ceramic nanoparticles on tribological properties of alumina sol–gel thin coatings*, Ceramics International, vol. 36, iss. 1, pp. 47-54, 2010, doi: 10.1016/j.ceramint.2009.06.024

[13] G. Ji, Z. Shi, W. Zhang, G. Zhao, *Tribological properties of titania nanofilms coated on glass surface by the sol–gel method*, Ceramics International, vol. 40, iss. 3, pp. 4655-4662, 2014, doi: 10.1016/j.ceramint.2013.09.006

[14] F. Alférez, J.J. Olaya, J. Bautista-Ruiz, *Síntesis y evaluación de resistencia a la corrosión de recubrimientos de SiO_2-TiO_2-ZrO_2-BiO_2 sobre acero inoxidable 316L producidos por sol-gel*, Boletín, de la Sociedad Española de Cerámica y Vidrio, vol. 57, iss. 5, pp. 195-206, 2018, doi. 10.1016/j.bsecv.2018.02.001

[15] S. Omar, F. Repp, P. Desimone, R. Weinkamer, W. Wagermaier, S. Ceré, J. Ballarre, *Sol–gel hybrid coatings with strontium-doped 45S5 glass particles for enhancing the performance of stainless steel implants: Electrochemical, bioactive and* in vivo *response*, Journal of Non-Crystalline Solids, vol. 425, pp. 1-10, 2015, doi: 10.1016/j.jnoncrysol.2015.05.024

[16] A. Marsal, F. Ansart, V. Turq, J.P. Bonino, J.M. Sobrino, Y.M. Chen, J. García, *Mechanical properties and tribological behavior of a silica or/and alumina coating prepared by sol-gel route on stainless steel,* Surface and Coatings Technology, vol. 237, pp. 234-240, 2013, doi: 10.1016/j.surfcoat.2013.06.037

[17] M.S. Kartavtseva, A.R. Kaul, T.V. Murzina, S.A. Savinov, A. Barthélémy, *$BiFeO_3$ thin films prepared using metalorganic chemical vapor deposition,* Thin Solid Films, vol. 515, iss. 16, pp. 6416-6421, 2007, doi: 10.1016/j.tsf.2006.11.133

[18] J. Bautista-Ruiz, *Caracterización Anticorrosiva y de Biocompatibilidad en Recubrimientos Silicio-Titanio-Zirconio Sintetizados Vía Sol-gel y Depositados sobre Sustratos de Acero Inoxidable*, Información Tecnológica, vol. 29, no. 1, pp. 201-210, 218, doi: 10.4067/S0718-07642018000100201

[19] S. Pourhashem, A. Afshar, *Double layer bioglass-silica coatings om 316L stainless steel by sol-gel method*, Ceramics International, vol. 40, iss. 1, pp. 993-1000, 2014, doi: 10.1016/j.ceramint.2013.06.096

[20] A. Owens, S. Brühl, S. Simison, C. Forsich, D. Heim, *Comparison of tribological properties of stainless steel with hard and soft DLC coatings*, Procedia Materials Science, vol. 9, pp. 246–253, 2015, doi: 10.1016/j.mspro.2015.04.031

[21] C. Lavollée, M. Gressier, J. García, J. Sobrino, J. Reby, M. Rossi, *New architectured hybrid sol-gel coatings for wear and corrosion protection of low-carbon steel*, Progress in Organic Coatings, vol. 99, pp. 337-345, 2016, doi: 10.1016/j.porgcoat.2016.06.015

[22] B. Pietrzyk, S. Miszczak, Ł. Kaczmarek, M. Klich, *Low friction nanocomposite aluminum oxide/MoS_2 coatings prepared by sol-gel method*, Ceramics International, vol. 47, iss. 7, pp. 8534-8539, 2018, doi: 10.1016/j.ceramint.2018.02.055

[23] A. Veber, Š. Kunej, D. Suvorov, *Synthesis and microstructural characterization of $Bi_{12}SiO_{20}$ (BSO) thin films produced by the sol-gel process*. Ceramics International, vol. 36, iss. 1, pp. 245-250, 2010, doi: 10.1016/j.ceramint.2009.07.024

[24] H. Gua, C. Dong, P. Chena, D. Bao, A. Kuang, X. Lic, *Growth of layered perovskite $Bi_4Ti_3O_{12}$thin films by sol–gel process,* Journal of Crystal Growth, vol. 186, iss. 3, pp. 403-408, 1998, doi: 10.1016/S0022-0248(97)00508-3

[25] W. Oliver, G. Pharr, *An Improved Technique for Determining Hardness and Elastic Modulus Using Load and Displacement Sensing Indentation Experiments*, Journal of Materials Research, vol. 7, iss. 6, pp. 1564–1583, 1992, doi: 10.1557/JMR.1992.1564